Published in final edited form as:
Neurosci Lett. 2014 June 27; 574: 70–75. doi:10.1016/j.neulet.2014.03.073.

Neuroprotective effect of aquaporin-4 deficiency in a mouse model of severe global cerebral ischemia produced by transient 4-vessel occlusion

Gökhan Akdemir[a,b,c], **Julien Ratelade**[a,b], **Nithi Asavapanumas**[a,b], and **A.S. Verkman**[a,b,*]

[a]Department of Medicine, University of California, San Francisco, CA 94143, USA

[b]Department of Physiology, University of California, San Francisco, CA 94143, USA

[c]Selçuk University, Medical Faculty, Department of Neurosurgery, Alaaddin Keykubat Campusö Selç uklu, Konya 42075, Turkey

Abstract

Astrocyte water channel aquaporin-4 (AQP4) facilitates water movement across the blood–brain barrier and into injured astrocytes. We previously showed reduced cytotoxic brain edema with improved neurological outcome in AQP4 knockout mice in water intoxication, infection and cerebral ischemia. Here, we established a 4-vessel transient occlusion model to test the hypothesis that AQP4 deficiency in mice could improve neurological outcome following severe global cerebral ischemia as occurs in cardiac arrest/resuscitation. Mice were subjected to 10-min transient bilateral carotid artery occlusion at 24 h after bilateral vertebral artery cauterization. Cerebral blood flow was reduced during occlusion by >94% in both $AQP4^{+/+}$ and $AQP4^{-/-}$ mice. The primary outcome, neurological score, was remarkably better at 3 and 5 days after occlusion in $AQP4^{-/-}$ than in $AQP4^{+/+}$ mice, and survival was significantly improved as well. Brain water content was increased by 2.8 ± 0.4% in occluded $AQP4^{+/+}$ mice, significantly greater than that of 0.3 ± 0.6% in $AQP4^{-/-}$ mice. Histological examination and immunofluorescence of hippocampal sections at 5 days showed significantly greater neuronal loss in the CA1 region of hippocampus in $AQP4^{+/+}$ than $AQP4^{-/-}$ mice. The neuroprotection in mice conferred by AQP4 deletion following severe global cerebral ischemia provides proof-of-concept for therapeutic AQP4 inhibition to improve neurological outcome in cardiac arrest.

Keywords

AQP4; Neuroprotection; Water transport; Astrocyte; Brain edema; Cerebral ischemia

1. Introduction

Aquaporin-4 (AQP4) is a water channel expressed at the plasma membrane in astrocytes throughout the central nervous system, where it functions as a bidirectional, water-selective

*Corresponding author at: 1246 Health Sciences East Tower, University of California, San Francisco, CA 94143-0521, USA. Tel.: +1 415 476 8530; fax: +1 415 665 3847. Alan.Verkman@ucsf.edu (A.S. Verkman). URL: http://www.ucsf.edu/verklab (A.S. Verkman).

transporter [1,2]. Evidence from knockout mice has implicated the involvement of AQP4 in water movement in brain and spinal cord, as well as in astrocyte migration and neuroexcitation (reviewed in [3]). In brain, AQP4 deletion in mice improves neurological outcome in models of cytotoxic (cell-swelling) brain edema, including acute water intoxication, ischemia and infection [4,5], which is explained by reduced water transport into brain tissue across the blood–brain barrier and reduced astrocyte swelling. However, AQP4 deletion in mice produces greater brain swelling and worsens neurological outcome in models of vasogenic (leaky-vessel) brain edema, including freeze-injury, brain tumor and brain abscess [6,7], as well as obstructive hydrocephalus [8], which is probably a consequence of reduced clearance of excess brain water.

AQP4 is a potential drug target, as inhibitors of AQP4 water transport function or expression may reduce cytotoxic edema in ischemic stroke, head trauma and some infections, and enhancers of AQP4 expression may reduce tumor-associated vasogenic edema [3]. AQP4 modulators may also reduce seizure activity in epilepsy and the local invasiveness of high-grade glioblastomas [7,9]. As cytotoxic brain swelling is an early pathogenic event in ischemic brain injury, we postulated that AQP4 inhibition may improve neurological outcome following transient focal ischemia, as in ischemic stroke, and global ischemia, as occurs in cardiac arrest/resuscitation and some neurological and cardiac surgical procedures. AQP4 knockout mice showed improved neurological outcome following permanent middle cerebral artery occlusion [4]. Mice inactivated for α-*syntrophin*, which manifest decreased astrocyte permeability due to a defect in AQP4 plasma membrane targeting, also showed protection following transient cerebral ischemia [10]. We recently showed improved survival in AQP4 knockout mice following transient bilateral carotid artery occlusion (BCAO) [11], which, on the basis of measurements of brain water accumulation and intracranial pressure, as well as studies of anoxia effects on brain slices, was attributed to reduced early brain water accumulation and astrocyte swelling. However, the limitations of the BCAO model included incomplete reduction in cerebral blood flow because of an intact vertebral artery circulation, and the reliance on mouse survival as a primary endpoint.

To extend these initial observations, here we established a 4-vessel occlusion mouse model to investigate whether the outcome of severe transient global cerebral ischemia, as occurs during cardiac arrest and resuscitation, would be benefitted by AQP4 deficiency. Permanent vertebral artery occlusion followed 24-h later by transient BCAO greatly reduced cerebral blood flow by >94% and produced marked neurological deficit and pathological changes in brain, which were remarkably less severe in AQP4 knockout mice.

2. Materials and methods

2.1. Mice

Experiments were done using male $AQP4^{+/+}$ and $AQP4^{-/-}$ mice (age 8–12 weeks; weight 25–30 g) in CD1 genetic backgrounds, which were generated as described [12]. Animal studies were approved by the University of California, San Francisco Committee on Animal Research (IACUC). Neurological scoring was assessed using a standard scoring system [13], with a maximum score of 12 (control mice) and minimum score of 0 for live but comatose

mice. Scoring included six factors: level of consciousness, corneal reflex, respirations, righting reflex, coordination and movement/activity, each scored 0, 1 or 2.

2.2. Four-vessel occlusion model

Mice were anesthetized using Avertin (2,2,2-tribromoethanol; 125 mg/kg, i.p.). After confirming deep anesthesia a midline incision was made in the dorsal neck and the cervical muscles were divided down to the atlanto-occipital junction. To produce experimental global cerebral ischemia, the alar foramina of the atlas were identified, and a monopolar microelectrode was passed in each foramina to electro-coagulate the underlying vertebral artery, and then the muscles and fascia were sutured closed in layers, as adapted from a previously reported rat model [14]. After 24 h a ventral mid-cervical horizontal skin incision was made in the anterior neck, and the thymus and sternocleidomastoid muscles were retracted to expose the common carotid arteries. Both carotid arteries were clipped at nearly the same time using a micro-clip applicator with lock (Fine Science Tools, Foster City, CA) with microserrefine clamp-curved/17 mm (jaw pressure 100 g) at the level of the middle sternocleidomastoid muscle. After 10 min occlusion time, both clips were removed by clip-forceps and the neck skin was sutured. Core body temperature was maintained at 36.5–37.5°Cusing a heat pad and overhead lamp. Mice were monitored for 8 h (breathing and ambulation) after the surgery and given buprenor-phine (0.1 mg/kg SC) as needed. For the survival study, mice were monitored twice a day.

2.3. Cerebral blood flow measurements

Mice were anesthetized and cortical cerebral blood flow (CBF) was measured in both hemispheres of $AQP4^{+/+}$ and $AQP4^{-/-}$ mice before occlusion, after vertebral artery occlusion, and after carotid artery occlusion. A midline scalp incision was made and CBF was measured through the skull using a non-invasive laser Doppler probe (Vasomedics, Minnesota, MN).

2.4. Analysis of brain vasculature

Mice were anesthetized and perfused in the left ventricle with10 mL of 50% carbon black ink and 4% paraformaldehyde. The brain was removed and the cerebral vasculature was photographed using a dissecting microscope.

2.5. Brain water content measurement

Mice were euthanized by anesthetic overdose and the brain was removed, weighed immediately (wet weight) and dried in a vacuum oven (Model 5851, NAPCO, Chicago, IL) at 121 °C for 24 h. The dried brains were re-weighed (dry weight). Brain water content was calculated as (wet weight − dry weight)/wet weight × 100.

2.6. Immunohistochemistry

Brains were removed at 5 days after the 4-vessel occlusion. Five micrometer-thick paraffin sections were immunostained as described [11] using the following antibodies: rabbit anti-AQP4 (1:200, Santa Cruz Biotechnology, Santa Cruz, CA), mouse anti-GFAP (1:200, Millipore, Temecula, CA), goat anti-myelin basic protein (MBP) (1:200, Santa Cruz

Biotechnology), rabbit anti-Iba1 (1:200, Wako, Richmond, VA), rat anti-CD45 (1:25, Pharmingen, BD Biosciences, Oxford, UK), goat anti-albumin (1:200 Santa Cruz Biotechnology) and mouse anti-NeuN (1:200, Millipore), followed by the appropriate fluorescent secondary antibody (1:200, Invitrogen, Carlsbad, CA) or biotinylated secondary antibody (1:500, Vector Laboratories, Burlingame, CA). Some sections were stained with hematoxylin and eosin. Tissue sections were examined with a Leica (Wetzlar, Germany) DM 4000 B microscope. Neuronal damage in CA1 region was quantified using the NeuN staining with the following score: 0: no damage; 1: between 0 and 25% damage; 2: between 25 and 50% damage; 3: between 50 and 75% damage; 4: >75% damage.

2.7. TTC staining

Brains from $AQP4^{+/+}$ and $AQP4^{-/-}$ mice were removed 5 days after 4-vessel occlusion and sectioned in cold phosphate buffered saline (PBS) into 2-mm thick coronal slices. Sections were incubated in 2% 2,3,5-triphenyltetrazolium chloride (TTC) in PBS at 37 °C for 30 min, washed in PBS, and fixed for 1 h in 4% paraformaldehyde (PFA).

2.8. Statistical analysis

Significance in cumulative survival studies was determined using the log-rank test. Other data were expressed as mean ± S.E. (generally 4–6 mice per each group). A significant difference was defined as $P < 0.05$. Group comparisons were made by one-way ANOVA with Scheffe's post hoc test or Student's *t*-test.

3. Results

3.1. 4-Vessel occlusion model of global cerebral ischemia

We modeled severe global cerebral ischemia in mice by transient 4-vessel occlusion in which permanent occlusion of the vertebral arteries was accomplished by cautery one day prior to transient bilateral occlusion of the carotid artery using surgical clips (Fig. 1A). Doppler analysis of CBF showed an ~18% reduction in blood flow just after vertebral artery occlusion (Fig. 1B). CBF was increased by ~14% over baseline at 24 h after vertebral artery occlusion. Transient bilateral carotid artery occlusion then reduced CBF by >94%, which was returned to approximately baseline level after reperfusion. Similar changes in CBF were seen in $AQP4^{+/+}$ and $AQP4^{-/-}$ mice. As shown in Fig. 1B (right), 2-vessel occlusion produced by transient bilaterial carotid artery occlusion alone resulted in a ~85% reduction in CBF.

Fig. 1C shows cerebrovascular anatomy as visualized following intracardiac ink perfusion. $AQP4^{+/+}$ and $AQP4^{-/-}$ mice have similar posterior communicating vasculature and no gross differences were seen between $AQP4^{+/+}$ and $AQP4^{-/-}$ mice.

3.2. Improved survival and neurological outcome in $AQP4^{-/-}$ mice following 4-vessel occlusion

Fig. 2A shows significantly improved survival of $AQP4^{-/-}$ mice than $AQP4^{+/+}$ mice after 4-vessel occlusion. $AQP4^{+/+}$ mice started to die at day 2 with ~50% of mice surviving to day 5, whereas the first death of an $AQP4^{-/-}$ mouse was seen at day 4 and ~80% of $AQP4^{-/-}$

mice were alive at day 5. Neurological outcome of surviving mice, as assessed using a standard neurological score (maximum score of 12 without neurological impairment), was significantly improved in the $AQP4^{-/-}$ mice, with fairly stable neurological scores from days 1–5 after 4-vessel occlusion (Fig. 2B). Vertebral artery occlusion produced a consistent mild ataxia in both $AQP4^{+/+}$ and $AQP4^{-/-}$ mice (neurological score reduced from 12 to 11), as expected, because of reduced cerebellar blood flow. Little further reduction in neurological score was seen in the $AQP4^{-/-}$ mice after the transient bilateral carotid artery occlusion.

We postulated that the improved survival and neurological outcome in $AQP4^{-/-}$ mice may be a consequence of reduced brain swelling. To assess brain edema, brain water content was measured from wet-to-dry weight ratios. Fig. 2C shows a significantly greater elevation in brain water content, by ~2.8% in the $AQP4^{+/+}$ mice than in $AQP4^{-/-}$ mice at 1 day after 4-vessel occlusion. Brain water content was slightly greater in $AQP4^{-/-}$ mice than in $AQP4^{+/+}$ mice at baseline, as noted previously [7], which may be related to mild extracellular space expansion in $AQP4^{-/-}$ mice [15]. Remarkably, no significant increase in brain water content was seen in the $AQP4^{-/-}$ mice following 4-vessel occlusion.

3.3. Reduced neuronal damage in $AQP4^{-/-}$ mice following 4-vessel occlusion

Neuronal damage was assessed in brain sections through hippocampus in control mice and in mice at 5 days after 4-vessel occlusion. Fig. 3A (top) shows hematoxylin and eosin-stained sections at low and high magnifications. As reported in prior studies of global ischemia, neuron damage manifests as condensation, fragmentation and dispersion of neuronal nuclei [16]. Immunofluorescence staining for neuronal marker NeuN is shown in Fig. 3A bottom. Areas with marked loss of NeuN staining were seen in mice undergoing 4-vessel occlusion, but not in control mice, with generally larger areas in the $AQP4^{+/+}$ mice. Fig. 3B summarizes pathology scores (score 0, no pathology) determined with sections from 5 mice. Mild neuronal pathology was seen at 1 day after 4-vessel occlusion, which was increased by 5 days, with significant greater pathology in the $AQP4^{+/+}$ mice.

TTC staining was also used to assess brain tissue viability, recognizing its limitations for studies in global ischemia in which, unlike in focal ischemia, it is not possible to compare ipsilateral and contralateral staining. Representative TTC-stained brain sections in Fig. 3C show areas of reduced staining, seen bilaterally, in $AQP4^{+/+}$ mice that were generally minimal in $AQP4^{-/-}$ mice and not seen in control untreated mice.

3.4. Assessment of astrocytes, myelin, inflammation and blood–brain barrier integrity

Immunofluorescence of brain sections was done to assess astrocytes, myelin, inflammation and blood–brain barrier integrity (Fig. 4). AQP4 expression was increased at 5 days after 4-vessel occlusion in $AQP4^{+/+}$ mice, which probably reflects the appearance of reactive astrocytes as found in prior studies of global cerebral ischemia [17]. AQP4 immunofluorescence was absent in $AQP4^{-/-}$ mice, as expected. GFAP, another astrocyte marker that is upregulated in reactive astrocytes, was also mildly increased following 4-vessel occlusion. Staining for myelin (MBP immunofluorescence) was similar in all conditions, confirming absence of demyelination in the global ischemia model used here.

Iba1 immunofluorescence was mildly increased following 4-vessel occlusion in AQP4$^{+/+}$ mice, which suggests mild intrinsic inflammation. However, infiltrating leukocytes, assessed with the marker CD45, were absent. At 5 days after 4-vessel occlusion blood–brain barrier integrity was intact as assessed by albumin extravasation.

4. Discussion

The main finding of this study was greatly improved survival and neurological outcome, as assessed by behavioral and histological criteria, in AQP4-deficient mice following transient 4-vessel global cerebral ischemia. The greatly reduced cerebral flow of >94% in our model more closely recapitulated the global ischemia associated with cardiac arrest/resuscitation than 2-vessel transient bilateral carotid artery occlusion used in our prior study [11]. In that study we also found improved survival and neurological outcome in AQP4-deficient mice, though the timing of animal mortality and details about occlusion times were different from the study here. Mechanistic analysis in the 2-vessel study supported the conclusion that reduced water permeability of the blood–brain barrier and astrocyte plasma membrane in AQP4 deficiency was responsible for improved outcome. Intracranial pressure after 2-vessel occlusion was much lower in AQP4-deficient mice, and brain slices from AQP4-deficient mice exposed to anoxia showed much less cell swelling than anoxia-exposed brain slices from wild-type mice as assessed by extracellular space volume measurement.

The data here and in our prior 2-vessel study suggest that reduced brain swelling in AQP4 deficiency, as a direct consequence of reduced astrocyte water permeability, is largely responsible for the improved neurological outcome. Cytotoxic brain swelling in anoxia is the consequence of cellular dysfunction leading to Na^+/K^+ pump failure, creating an osmotic gradient that drives water influx [18]. Astrocyte swelling is one of the earliest manifestations of anoxia in brain tissue [19]. As a consequence of astrocyte swelling there is increased extracellular space K^+ and glutamate, as well as blood–brain barrier dysfunction and cytokine-driven local inflammation, which together contribute to a positive-feedback cycle resulting in neuronal injury [20,21]. We previously found improved outcome in other models of cytotoxic brain edema, including acute water intoxication, in which osmotic brain swelling occurs in response to serum hyponatremia, and in focal ischemic stroke produced by permanent middle cerebral artery occlusion [4]. Interruption of the astrocyte swelling response by AQP4 inhibition or down-regulation may thus have therapeutic benefit in preserving brain tissue and improving neurological outcome in severe global cerebral ischemia and in other brain injuries associated with cytotoxic swelling.

The results here and in prior studies showing neuroprotection in cytotoxic brain edema support the development of small-molecule inhibitors of AQP4 water permeability. Unfortunately, as reviewed recently [3], progress has been slow in identification of suitable compounds. Though several compounds were reported to inhibit AQP4 water permeability, including anti-epileptics [22], carbonic anhydrase inhibitors [23], and tetraethylammonium [24], subsequent studies failed to confirm AQP4 inhibition [25]. Perhaps further screening of diverse compound collections and biased libraries, based on AQP4 crystal structure data [26], may yield AQP4inhibitors. There will be a number of challenges in AQP4 inhibitor

therapy, including the need for blood–brain barrier penetration and AQP4 selectivity, as there are 13 mammalian aquaporins, many having a broad tissue distribution.

In conclusion, targeted AQP4 gene deletion in mice remarkably improved survival and neurological outcome following severe global cerebral ischemia in a 4-vessel occlusion model. These results support prior studies showing improve outcomes in AQP4 deficiency in mouse models of cytotoxic brain and spinal cord swelling, and provide compelling proof-of-concept for identification and testing of small-molecule AQP4 inhibitors. An important caveat should be noted, however, that conclusions from neuroprotection studies done in mice should be extrapolated to humans with great caution, as effective therapeutics in mice are often not effective in human clinical trials.

Acknowledgments

This work was supported by grants DK35124, EY13574, EB00415 and DK72517 from the National Institutes of Health and grants from the Guthy-Jackson Charitable Foundation.

References

1. Frigeri A, Gropper MA, Umenishi F, Kawashima M, Brown D, Verkman AS. Localization of MIWC and GLIP water channel homologs in neuromuscular, epithelial and glandular tissues. J. Cell Sci. 1995; 108(Pt 9):2993–3002. [PubMed: 8537439]
2. Nielsen S, Nagelhus EA, Amiry-Moghaddam M, Bourque C, Agre P, Otterse OP. Specialized membrane domains for water transport in glial cells: high-resolution immunogold cytochemistry of aquaporin-4 in rat brain. J. Neurosci. 1997; 17:171–180. [PubMed: 8987746]
3. Papadopoulos MC, Verkman AS. Aquaporin water channels in the nervous system. Nat. Rev. Neurosci. 2013; 14:265–277. [PubMed: 23481483]
4. Manley GT, Fujimura M, Ma T, Noshita N, Filiz F, Bollen AW, Chan P, Verkman AS. Aquaporin-4 deletion in mice reduces brain edema after acute water intoxication and ischemic stroke. Nat. Med. 2000; 6:159–163. [PubMed: 10655103]
5. Papadopoulos MC, Verkman AS. Aquaporin-4 gene disruption in mice reduces brain swelling and mortality in pneumococcal meningitis. J. Biol. Chem. 2005; 280:13906–13912. [PubMed: 15695511]
6. Bloch O, Papadopoulos MC, Manley GT, Verkman AS. Aquaporin-4 gene deletion in mice increases focal edema associated with staphylococcal brain abscess. J. Neurochem. 2005; 95:254–262. [PubMed: 16181429]
7. Papadopoulos MC, Manley GT, Krishna S, Verkman AS. Aquaporin-4 facilitates reabsorption of excess fluid in vasogenic brain edema. FASEB J. 2004; 18:1291–1293. [PubMed: 15208268]
8. Bloch O, Auguste KI, Manley GT, Verkman AS. Accelerated progression of kaolin-induced hydrocephalus in aquaporin-4-deficient mice. J. Cereb. Blood Flow Metab. 2006; 26:1527–1537. [PubMed: 16552421]
9. Binder DK, Yao X, Zador Z, Sick TJ, Verkman AS, Manley GT. Increased seizure duration and slowed potassium kinetics in mice lacking aquaporin-4 water channels. Glia. 2006; 53:631–636. [PubMed: 16470808]
10. Amiry-Moghaddam M, Otsuka T, Hurn PD, Traystman RJ, Haug FM, Froehner SC, Adams ME, Neely JD, Agre P, Ottersen OP, Bhardwaj A. An alpha-syntrophin-dependent pool of AQP4 in astroglial end-feet confers bidirectional water flow between blood and brain. Proc. Natl. Acad. Sci. U. S. A. 2003; 100:2106–2111. [PubMed: 12578959]
11. Katada R, Akdemir G, Asavapanumas N, Ratelade J, Zhang H, Verkman AS. Greatly improved survival and neuroprotection in aquaporin-4-knockout mice following global cerebral ischemia. FASEB J. 2014; 28:705–714. [PubMed: 24186965]

12. Ma T, Yang B, Gillespie A, Carlson EJ, Epstein CJ, Verkman AS. Generation and phenotype of a transgenic knockout mouse lacking the mercurial-insensitive water channel aquaporin-4. J. Clin. Invest. 1997; 100:957–962. [PubMed: 9276712]
13. Abella BS, Zhao D, Alvarado J, Hamann K, Vanden Hoek TL, Becker LB. Intra-arrest cooling improves outcomes in a murine cardiac arrest model. Circulation. 2004; 109:2786–2791. [PubMed: 15159295]
14. Pulsinelli WA, Brierley JB. A new model of bilateral hemispheric ischemia in the unanesthetized rat. Stroke. 1979; 10:267–272. [PubMed: 37614]
15. Yao X, Hrabetova S, Nicholson C, Manley GT. Aquaporin-4-deficient mice have increased extracellular space without tortuosity change. J. Neurosci. 2008; 28:5460–5464. [PubMed: 18495879]
16. Harukuni I, Bhardwaj A. Mechanisms of brain injury after global cerebral ischemia. Neurol. Clin. 2006; 24:1–21. [PubMed: 16443127]
17. Petito CK, Morgello S, Felix JC, Lesser ML. The two patterns of reactive astrocytosis in postischemic rat brain. J. Cereb. Blood Flow Metab. 1990; 10:850–859. [PubMed: 2211878]
18. Simard JM, Kent TA, Chen M, Tarasov KV, Gerzanich V. Brain oedema in focal ischaemia: molecular pathophysiology and theoretical implications. Lancet Neurol. 2007; 6:258–268. [PubMed: 17303532]
19. Garcia JH, Kalimo H, Kamijyo Y, Trump BF. Cellular events during partial cerebral ischemia. I. Electron microscopy of feline cerebral cortex after middle-cerebral-artery occlusion. Virchows Arch. B Cell Pathol. 1977; 25:191–206. [PubMed: 413252]
20. Dirnagl U, Iadecola C, Moskowitz MA. Pathobiology of ischaemic stroke: an integrated view. Trends Neurosci. 1999; 22:391–397. [PubMed: 10441299]
21. Moskowitz MA, Lo EH, Iadecola C. The science of stroke: mechanisms in search of treatments. Neuron. 2010; 67:181–198. [PubMed: 20670828]
22. Huber VJ, Tsujita M, Kwee IL, Nakada T. Inhibition of aquaporin 4 by antiepileptic drugs. Bioorg. Med. Chem. 2009; 17:418–424. [PubMed: 18178093]
23. Huber VJ, Tsujita M, Yamazaki M, Sakimura K, Nakada T. Identification of arylsulfonamides as aquaporin 4 inhibitors. Bioorg. Med. Chem. Lett. 2007; 17:1270–1273. [PubMed: 17178220]
24. Detmers FJ, de Groot BL, Muller EM, Hinton A, Konings IB, Sze M, Flitsch SL, Grubmüller H, Deen PM. Quaternary ammonium compounds as water channel blockers. Specificity, potency, and site of action. J. Biol. Chem. 2006; 2(81):14207–14214. [PubMed: 16551622]
25. Yang B, Zhang H, Verkman AS. Lack of aquaporin-4 water transport inhibition by antiepileptics and arylsulfonamides. Bioorg. Med. Chem. 2008; 16:7489–7493. [PubMed: 18572411]
26. Ho JD, Yeh R, Sandstrom A, Chorny I, Harries WE, Robbins RA, Miercke LJ, Stroud RM. Crystal structure of human aquaporin 4 at 1.8 A and its mechanism of conductance. Proc. Natl. Acad. Sci. U. S. A. 2009; 106:7437–7442. [PubMed: 19383790]

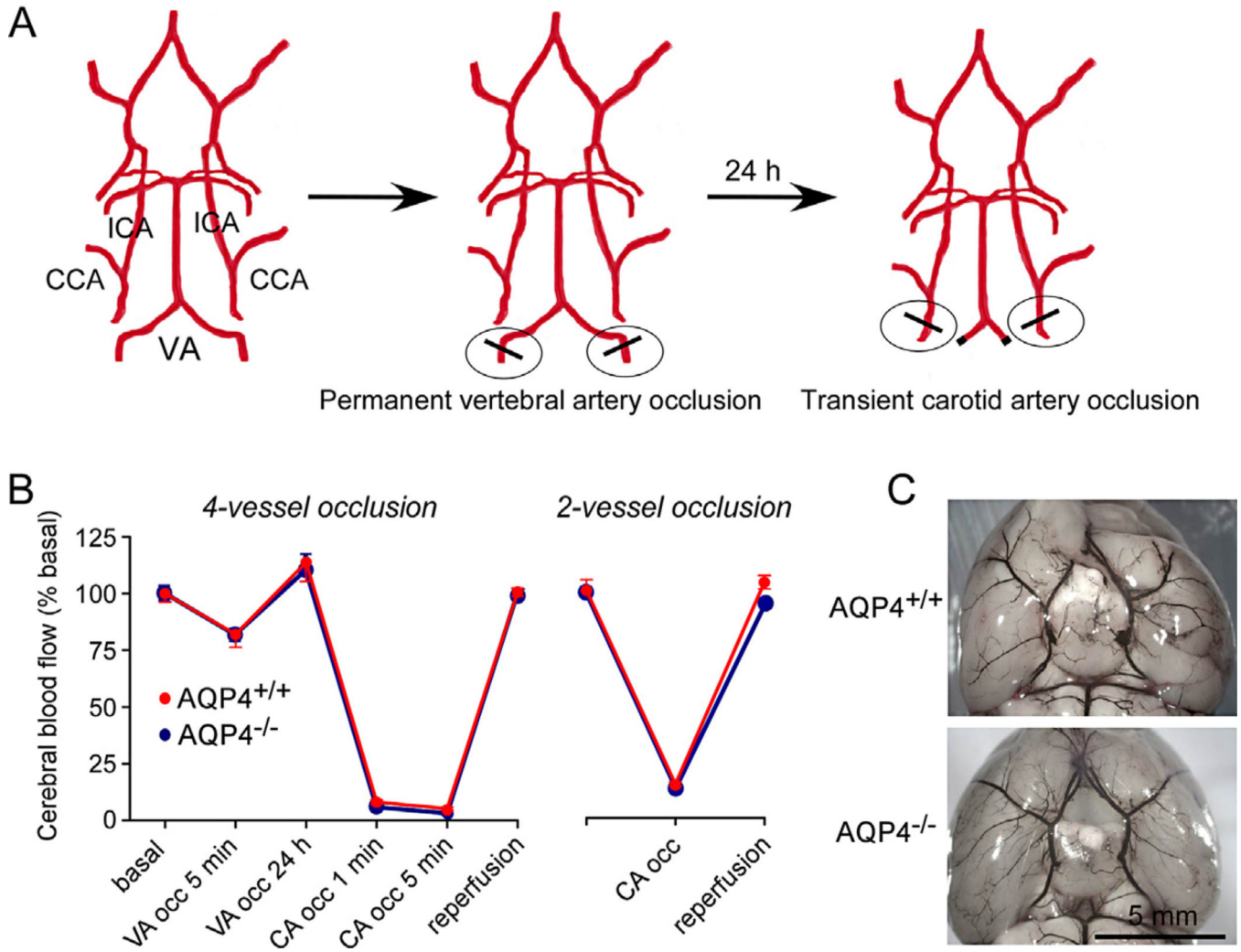

Fig. 1.

4-Vessel occlusion model of severe global cerebral ischemia in mice. (A) Diagram of approach showing permanent vertebral artery (VA) occlusion produced by cautery at 24 h before transient bilateral common carotid artery (CCA) occlusion. ICA: internal carotid artery. (B) Cerebral blood flow measured by Doppler at indicated times in 4-vessel (left) and 2-vessel (right) models (mean ± S.E., 4 mice per group). (C) Cerebrovascular anatomy visualized following intravenous ink injection.

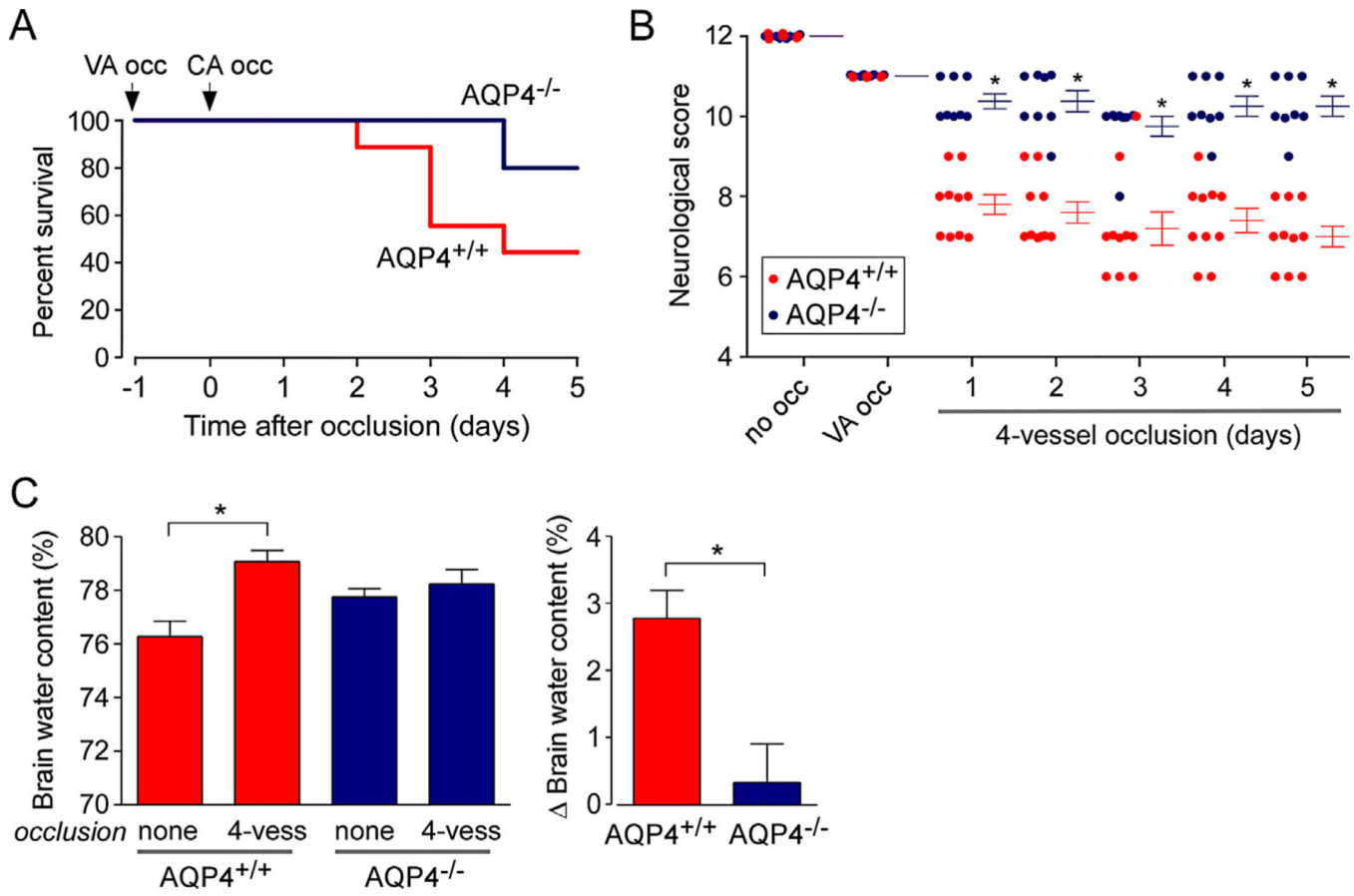

Fig. 2.

Improved survival and neurological outcome of AQP4-deficient mice following 4-vessel occlusion. (A) Survival plot from 12 $AQP4^{+/+}$ and 12 $AQP4^{-/-}$ mice undergoing 10-min bilateral carotid artery occlusion 24 h after permanent vertebral artery occlusion. Survival was significantly different with $P < 0.05$ (log-rank test). (B) Neurological score (see Section 2, score 12 without neurological impairment) shown for individual mice from study in A (S.E., $*P < 0.05$). (C) Brain water content determined from wet-to-dry weight ratios for control mice and mice at 1 day after 4-vessel occlusion (S.E., 6 mice per group, $*P < 0.05$).

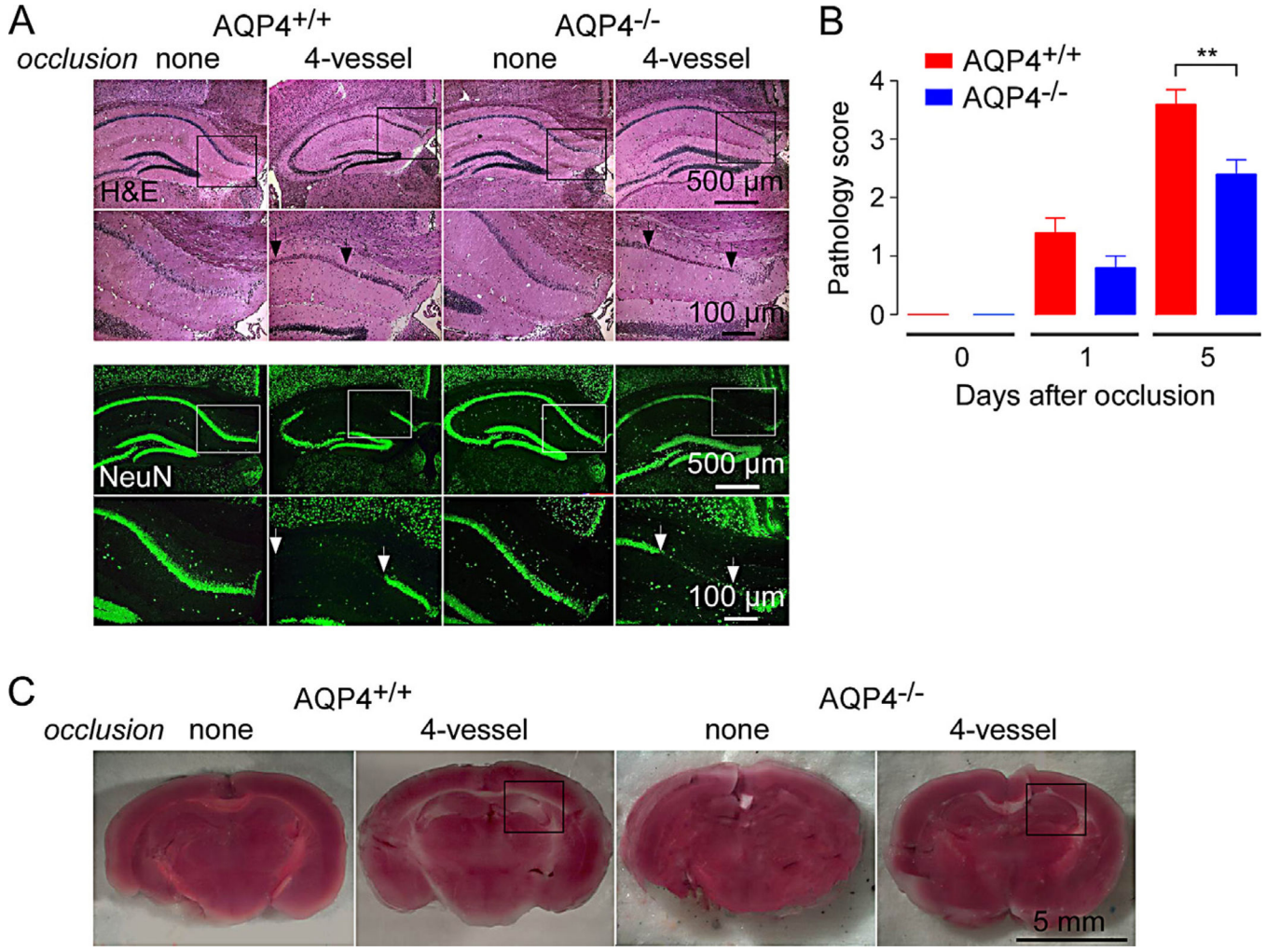

Fig. 3.

Reduced neuronal injury in AQP4-deficient mice following 4-vessel occlusion. (A) Hematoxylin and eosin-stained sections through hippocampus in control mice and at 5 days after 4-vesssel occlusion (top). Higher magnification of boxed areas shown. NeuN (neuronal marker) immunofluorescence (bottom). Micrographs representative of 5 mice studied per condition. (B) Pathological score (see Methods, score 0 without pathology) deduced from analysis of hippocampal sections (S.E., 5 mice per group, $^{**}P < 0.05$). (C) TTC staining of freshly cut brain of control mice and at 5 days after 4-vessel occlusion. Hippocampus region indicated by box. Representative of TTC staining from 5 mice.

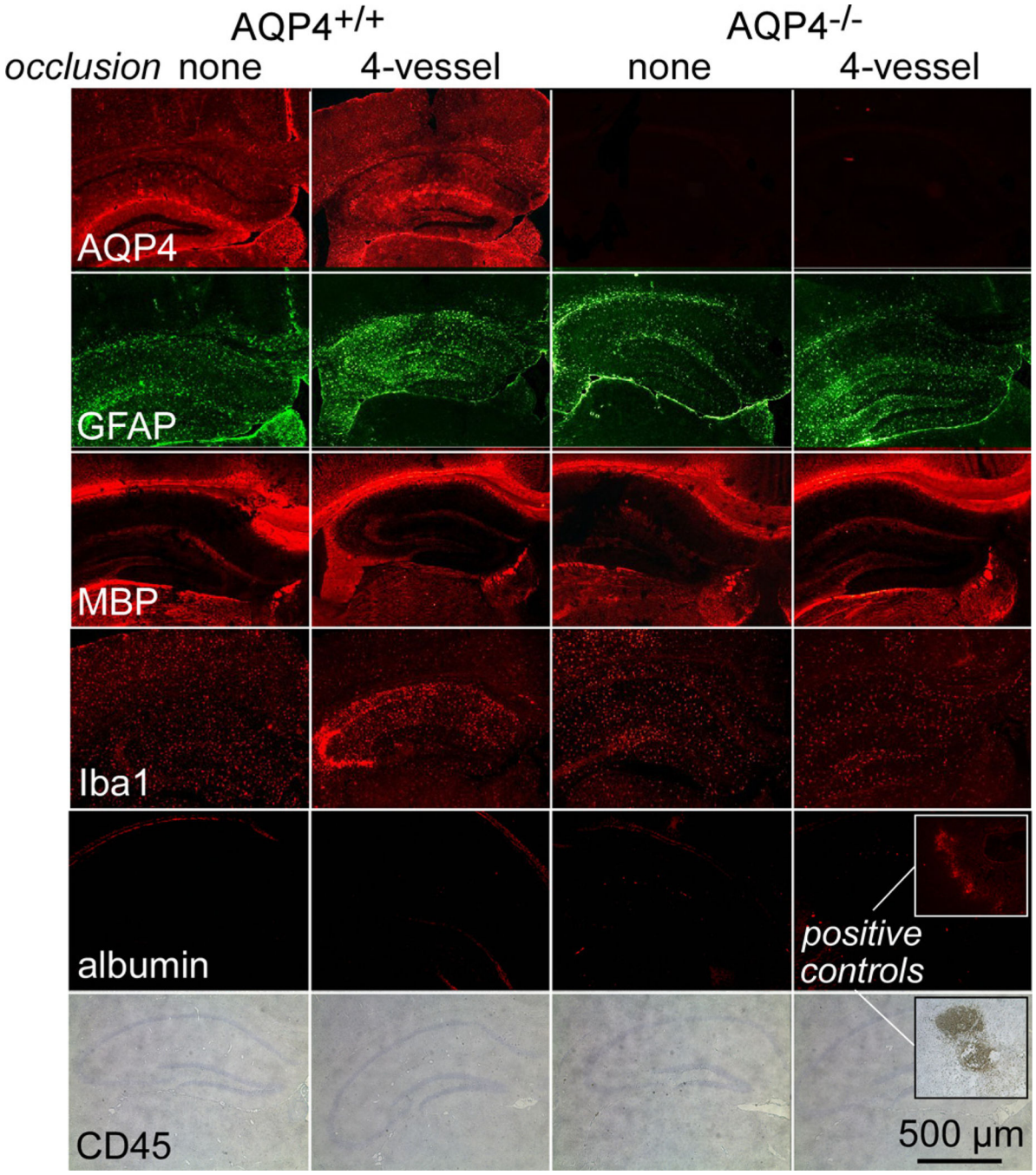

Fig. 4.

Assessment of astrocytes, myelin, inflammation and blood–brain barrier integrity following 4-vessel occlusion. Immunostaining of brain sections in control mice and at 5 days after 4-vessel occlusion with stains for astrocytes (AQP4 and GFAP), myelin (MBP), microglia (Iba1), infiltrating leukocytes (CD45) and blood–brain barrier integrity (albumin). Micrographs are representative of 5 mice per group.